

Controlling Groups of Mobile Beamformers

Nikolaos Chatzipanagiotis, Yupeng Liu, Athina Petropulu and Michael M. Zavlanos

Abstract—In this paper, we address the problem of controlling networks of wireless mobile nodes to propagate information over large distances, while minimizing power consumption and maintaining desired Quality of Service (QoS) guarantees. For this, we rely on collaborative beamforming, where groups of nodes collaborate to adjust the initial phase of their transmitted signals to form a beam that focuses on the direction of a desired destination. This allows for transmission over large distances, minimizes multiuser interference and also provides significant power savings, which increases network longevity. Beamforming has been thoroughly studied in the networking literature in the context of stationary antennas. The contribution of this work is a novel framework that jointly optimizes the beamforming weights and node positions in networks of mobile beamformers. In particular, a hybrid control scheme is proposed, in which optimal beamforming is integrated with potential-field-based motion control, designed to optimize power consumption in the space of node positions, while ensuring QoS. The integrated system is shown to exhibit superior performance in terms of power savings compared to approaches that do not consider node mobility. This makes our approach very promising for further research and applications in mobile wireless networks.

I. INTRODUCTION

Mobile robot networks have been recently proposed for a variety of applications ranging from exploration, environmental sampling, surveillance and reconnaissance, to cooperative construction and manipulation. Information sharing among network members or data routing to specified base stations for processing, plays a vital role in such schemes [1], [2]. This restricts collective robot motion to formations that guarantee reliability of the communication network, and induces an interplay between the physical constraints on the robot trajectories and velocities, and the optimization of communication variables like signal-to-interference-plus-noise-ratio (SINR) and transmitted powers. In this paper we propose a novel algorithm to address this interplay that relies on collaborative beamforming for optimal communications.

Modeling wireless communications in multi-robot systems has typically relied on constructs from graph theory, wherein proximity-based graphs have been repeatedly used to capture multi-hop communications, with disc-based and weighted-link models gaining the most popularity. This is consistent with early approaches to wireless networking that used disk models to abstract the physical layer [3], [4]. As a result, attempts to manipulate multi-hop communication in

This work is supported in part by the National Science Foundation under Grant CNS #1054604.

Nikolaos Chatzipanagiotis and Michael M. Zavlanos are with the Dept. of Mechanical Engineering, Duke University, Durham, NC, 27708, USA {n.chatzip,michael.zavlanos}@duke.edu. Yupeng Liu and Athina Petropulu are with the Dept. of Electrical and Computer Engineering, Rutgers University, Piscataway, NJ 08648, USA {ypliu,athinap}@rutgers.edu.

networked systems have mostly relied on controlling the connectivity of the underlying dynamic graphs. They can be classified into those that increase network connectivity [5]–[7] and less restrictive ones that allow links to be lost [8]–[10]. To address the somewhat arbitrary association of links with arcs on a graph [11], recently, weighted graph models were proposed, where the weights capture the packet error probability of each link [12]–[14], allowing to model routing and scheduling problems as optimization problems that accept link reliabilities as inputs.

Although multi-hop networks possess well known advantages, such as their ability to relay information over long distances and distribute computation over their nodes, real-time transmissions over multiple hops tend to suffer from long delays, large number of packet collisions and interference, especially so for the case of ad hoc networks [15]. A preferred solution to these issues is *collaborative* (or distributed) *beamforming*, where groups of nodes collaborate to adjust the phase of their transmitted signals to form a beam that focuses on the direction of the desired destination. This process increases the directional channel gain [16], [17], enabling long distance transmissions with lower power and fewer hops, minimizing thus interference [11], [15].

In this paper, we consider networks of mobile beamformers that relay information between a set of source nodes and their assigned destinations. As in beamforming for stationary nodes [18]–[20], the mobile beamformers amplify-and-forward (AF) signals from the sources in order to take advantage of constructive interference effects at the destinations' locations. The contribution of this work is to exploit the dependence of optimal beamforming on the node positions in order to further increase system performance. We propose a hybrid control scheme, where optimal beamforming is integrated with potential-field-based motion control designed to optimize power consumption in the space of node positions, while ensuring QoS. The integrated system is shown to exhibit significant power savings compared to approaches that do not consider node mobility.

The rest of this paper is organized as follows. In section II we present the beamforming algorithm for a stationary relay network. In section III we consider mobile relays, develop motion controllers for the nodes and integrate them with optimization of the beamforming variables in a hybrid control scheme. Finally, in section IV we present numerical results to illustrate the effectiveness of our approach.

II. SYSTEM MODEL & PROBLEM DEFINITION

Consider a network composed of M source-destination pairs of single antenna nodes, where we assume that due to

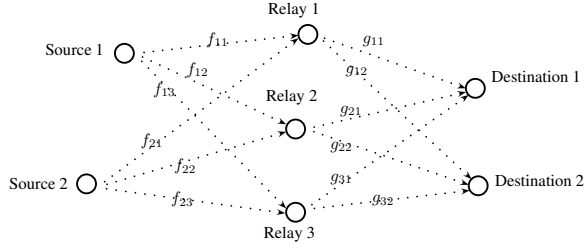


Fig. 1. Collaborative beamforming between 2 source-destination pairs via 3 relays. The signal transmitted from source 1 is intended for destination 1, while the signal transmitted from source 2 is intended for destination 2. Signals from sources 1 and 2 that reach destinations 2 and 1, respectively, are considered interference. Shown are also the channel gains f_{ij} between sources and relays and g_{ij} between relays and destinations.

large fading effects direct links between source and destination antennas are negligible, such that effective communication requires collaboration with a group of K dedicated, single-antenna relay nodes. The process of *collaborative beamforming* utilizes an AF transmission scheme, during which the relay antennas retransmit an amplified and phase-steered version of the received source signals, by multiplying them with appropriate weights (linear precoders). This leads to significant reduction in power consumption for each node and also reduces interference, by enabling space-division multiple access (SDMA).

In this paper, we assume that a central station has access to the second order statistics of channel state information, which it uses to compute the beamforming weights and then distribute them to the relay antennas via a dedicated channel. As shown in [20], during the first communication stage, every source i transmits the signal $\sqrt{P_0}s_i$, where P_0 is the common, source-transmit power and s_i , $i = 1, \dots, M$ denote the information symbols, modeled as independent identically distributed (i.i.d.) Gaussian random variables with zero mean and unit variance $\mathcal{N}(0, 1)$. The received signal at every relay j is given by

$$r_j = \sqrt{P_0} \sum_{i=1}^M f_{ij} s_i + n_j,$$

where $n_j \in \mathbb{C}$ is a circularly symmetric, complex Gaussian random noise, i.e. $n_j \sim \mathcal{CN}(0, 1)$. Correspondingly, the received signal vector at all relays is

$$\mathbf{r} = \sqrt{P_0} \mathbf{F} \mathbf{s} + \mathbf{n}, \quad (1)$$

where $\mathbf{s} = [s_1, \dots, s_M]^T \in \mathbb{R}^M$, $\mathbf{r} = [r_1, \dots, r_K]^T \in \mathbb{C}^K$, $\mathbf{n} = [n_1, \dots, n_K]^T \in \mathbb{C}^K$ and

$$\mathbf{F} = \begin{bmatrix} f_{11} & \dots & f_{M1} \\ \vdots & \ddots & \vdots \\ f_{1K} & \dots & f_{MK} \end{bmatrix} = [\mathbf{f}_1 \quad \dots \quad \mathbf{f}_M] \in \mathbb{C}^{K \times M}$$

is a channel state matrix, with $\mathbf{f}_i = [f_{i1}, \dots, f_{iK}]^T \in \mathbb{C}^K$ denoting the channel gain column vector from source i to all relays. $(\cdot)^T$ denotes the transposition operation.

During the second communication stage, the relays retransmit, in an AF fashion, a linear transformation of \mathbf{r} , i.e.,

$$\mathbf{t} = \mathbf{W} \mathbf{r} = \sqrt{P_0} \mathbf{W} \mathbf{F} \mathbf{s} + \mathbf{W} \mathbf{n}, \quad (2)$$

where $\mathbf{t} \in \mathbb{C}^K$ denotes the forwarded signal vector and $\mathbf{W} \in \mathbb{C}^{K \times K}$ is the beamforming matrix. By similar reasoning as above, the received signal vector $\mathbf{h} \in \mathbb{C}^M$ at the destinations equals

$$\mathbf{h} = \sqrt{P_0} \mathbf{G} \mathbf{W} \mathbf{F} \mathbf{s} + \mathbf{G} \mathbf{W} \mathbf{n} + \mathbf{z}, \quad (3)$$

where $\mathbf{z} = [z_1, \dots, z_M]^T \in \mathbb{C}^M$ denotes the vector stacking circularly symmetric, complex Gaussian random noise components at destinations and

$$\mathbf{G} = \begin{bmatrix} g_{11} & \dots & g_{K1} \\ \vdots & \ddots & \vdots \\ g_{1M} & \dots & g_{KM} \end{bmatrix} = [\mathbf{g}_1^T \quad \dots \quad \mathbf{g}_M^T]^T \in \mathbb{C}^{M \times K}$$

is a channel state matrix, with $\mathbf{g}_i = [g_{1i}, \dots, g_{Ki}]^T \in \mathbb{C}^K$ denoting the channel gain column vector from all relay antennas to destination i . This process is shown in Fig. 1. Based on this model, the sum transmit power at the relays is calculated as

$$P_T = \mathbb{E}\{\|\mathbf{t}\|_F^2\} = \text{Tr}(P_0 \mathbf{W} \mathbf{F} \mathbf{F}^H \mathbf{W}^H) + \text{Tr}(\mathbf{W} \mathbf{W}^H), \quad (4)$$

where $\|\cdot\|_F$ denotes the Frobenius norm, $\mathbb{E}(\cdot)$ accounts for expectation with respect to time and $(\cdot)^H$ is the operation of conjugate transposition. Also, the instantaneous SINR at every destination i equals

$$\text{SINR}_i = \frac{P_0 |\mathbf{g}_i^T \mathbf{W} \mathbf{f}_i|^2}{P_0 \sum_{m=1, \dots, M}^{m \neq i} |\mathbf{g}_i^T \mathbf{W} \mathbf{f}_m|^2 + \|\mathbf{g}_i^T \mathbf{W}\|^2 + 1}, \quad (5)$$

where the term $P_0 \sum_{m=1, \dots, M}^{m \neq i} |\mathbf{g}_i^T \mathbf{W} \mathbf{f}_m|^2$ represents interference at destination i caused by signals intended for other destinations and $|\cdot|$ denotes the magnitude of a complex number. The objective in distributed beamforming is to find the optimal beamforming weights \mathbf{W} that minimize the total transmitted power at the relays subject to specified SINR bounds $\gamma_i > 0$ at the destinations, i.e.,

$$\begin{aligned} \min_{\mathbf{W}} \quad & P_T(\mathbf{W}) \\ \text{s.t.} \quad & \text{SINR}_i(\mathbf{W}) \geq \gamma_i, \quad \forall i = 1, \dots, M. \end{aligned} \quad (6)$$

A. Collaborative Beamforming

Since every relay node carries a single antenna, \mathbf{W} is a diagonal matrix, which enables us to express the sum transmit power in (4) as

$$P_T = \mathbf{w}^H \mathbf{R}_T \mathbf{w} \quad (7)$$

where $\mathbf{w} = [[\mathbf{W}]_{11}, \dots, [\mathbf{W}]_{KK}]^T \in \mathbb{C}^K$ is a column vector containing all the diagonal elements of \mathbf{W} , with $[\mathbf{W}]_{jj}$ denoting the beamforming weight that relay node j applies on its signal to be forwarded, and $\mathbf{R}_T = \mathbf{I}_K + P_0 \text{diag}\left\{\sum_{i=1, \dots, M} \mathbb{E}\{|f_{i1}|^2\}, \dots, \sum_{i=1, \dots, M} \mathbb{E}\{|f_{iK}|^2\}\right\}$. Similarly, we can manipulate the expression in (5) to express the average SINR as

$$\text{SINR}_i = \frac{P_0 \mathbf{w}^H \mathbf{R}_S^{(i)} \mathbf{w}}{P_0 \mathbf{w}^H \mathbf{R}_I^{(i)} \mathbf{w} + \mathbf{w}^H \mathbf{R}_n^{(i)} \mathbf{w} + 1}, \quad (8)$$

with $\mathbf{R}_S^{(i)} = \mathbb{E}\{(\mathbf{f}_i^* \odot \mathbf{g}_i^*)(\mathbf{f}_i^T \odot \mathbf{g}_i^T)\}$, $\mathbf{R}_I^{(i)} = \sum_{m=1, \dots, M}^{m \neq i} \mathbb{E}\{(\mathbf{f}_m^* \odot \mathbf{g}_i^*)(\mathbf{f}_m^T \odot \mathbf{g}_i^T)\}$ and $\mathbf{R}_n^{(i)} =$

$\text{diag}\{\mathbb{E}\{|g_{1i}|^2\}, \dots, \mathbb{E}\{|g_{Ki}|^2\}\}$, where $(\cdot)^*$ stands for the conjugation operation and \odot denotes the Schur (entrywise) product. With the above notation, we can equivalently write the optimization problem (6) as

$$\begin{aligned} \min_{\mathbf{w}} \quad & \mathbf{w}^H \mathbf{R}_T \mathbf{w} \\ \text{s.t.} \quad & \mathbf{w}^H \mathbf{Q}^{(i)} \mathbf{w} \geq 1, \quad \forall i = 1, \dots, M, \end{aligned} \quad (9)$$

where $\mathbf{Q}^{(i)} = \frac{P_0}{\gamma_i} \mathbf{R}_S^{(i)} - P_0 \mathbf{R}_I^{(i)} - \mathbf{R}_n^{(i)}$ and it is not difficult to see that it is a Hermitian matrix.

The matrices $\mathbf{Q}^{(i)}$ are, in general, indefinite and therefore optimization problem (9) falls into the category of nonconvex, quadratic, quadratically constrained programming problems, which, in general, are NP-hard to solve. Nevertheless, by defining the variable $\mathbf{X} \triangleq \mathbf{w} \mathbf{w}^H$ [21] we can express (9) in the equivalent form

$$\begin{aligned} \min_{\mathbf{X}} \quad & \text{Tr}(\mathbf{X} \mathbf{R}_T) \\ \text{s.t.} \quad & \text{Tr}(\mathbf{X} \mathbf{Q}^{(i)}) \geq 1, \quad \forall i = 1, \dots, M \\ & \mathbf{X} \in \mathbb{S}_+^K, \\ & \text{rank}(\mathbf{X}) = 1 \end{aligned} \quad (10)$$

where $\mathbf{X} \in \mathbb{S}_+^K$ imposes the (convex) constraint that matrix \mathbf{X} belongs to the cone of symmetric, positive semidefinite matrices of dimension K . Problem (10) is still nonconvex because of the rank constraint, however, dropping the rank constraint, a suboptimal solution [21] can be obtained by solving the relaxation

$$\begin{aligned} \min_{\mathbf{X}} \quad & \text{Tr}(\mathbf{X} \mathbf{R}_T) \\ \text{s.t.} \quad & \text{Tr}(\mathbf{X} \mathbf{Q}^{(i)}) \geq 1, \quad \forall i = 1, \dots, M \\ & \mathbf{X} \in \mathbb{S}_+^K, \end{aligned} \quad (11)$$

which is a semidefinite programming problem and can be efficiently solved by interior point methods [22]. Due to the relaxation, the optimizer \mathbf{X}^* of (11) will not be rank one in general. If it is, then it will be the optimal solution to the original problem (10). If not, randomization techniques [23] can be employed to obtain a rank one matrix.

B. Modeling wireless channels

In this paper, the transmitted signals are considered narrowband and a flat fading model is assumed, which is a reasonable assumption in current robotic applications where the transmission rates are low enough. Since exact characterization of wireless channels is extremely challenging, owing to their time-varying and unpredictable nature, a typically used approximation models channels as multi-scale dynamical systems with two major dynamics: *small-scale (multipath) fading* accounting for the variation of signal strength over distances of the order of the carrier wavelength, due to constructive and destructive interference of multiple signal paths, and *large-scale fading (path loss and shadowing)* accounting for signal attenuation due to free space propagation of signal and shadowing by large objects, such as walls. Based on this, the baseband equivalent channel gain $c_{ij} \in \mathbb{C}$ between transmitter i and receiver j can be approximated by

$$c_{ij} = \alpha_{ij} \beta_{ij} e^{j(2\pi/\lambda)d_{ij}}, \quad (12)$$

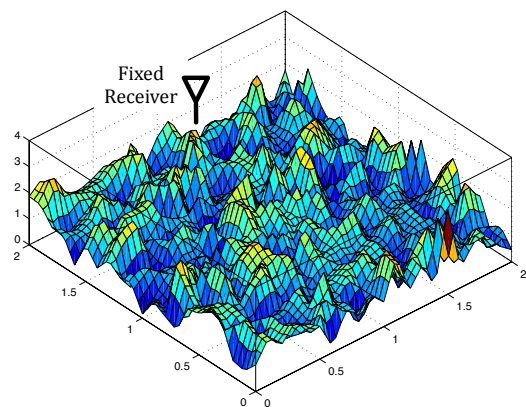


Fig. 2. Spatial map that returns the Rayleigh distributed channel gain α_{ij} due to multipath fading at arbitrary positions of the transmitter i , given a fixed position of the receiver j . The environment is assumed square and scattering-rich, and the channel is sampled independently for positions of the transmitter i that fall on the vertices of a square grid that are half a wavelength apart. Cubic interpolation is performed to model correlations of the channel gains for positions of the transmitter i that lie in-between grid vertices (closer than half a wavelength apart). Similar maps can be obtained for fixed transmitters.

where α_{ij} captures multipath fading, β_{ij} captures path loss, λ denotes the wavelength of carrier waves and d_{ij} denotes the Euclidean distance between nodes i and j .

A typical assumption for rich scattering environments, that also works well in practice [24], is to take the gain $\alpha_{ij} \sim \mathcal{CN}(0, 1/2)$, as per the Rayleigh distribution.¹ Further, we assume that α_{ij} is independent from α_{kj} for nodes i and k that are more than half a wavelength apart. By enforcing transmitting antennas to move sufficiently slow, we can also render Doppler shift effects negligible [24]. On the other hand, the path loss coefficient is a function of distance between the antennas given by $\beta_{ij} = d_{ij}^{-\mu/2}$, where μ is the path loss exponent and represents the power fall-off rate. Note that we consider the environment to be obstacle-free and, thus, large-scale shadowing effects are not included in expression (12).

Remark 2.1 (Multipath fading map): As hinted before, small-scale effects captured in the gain α_{ij} vary spatially with respect to the configuration of the transmit and receive antennas i and j , respectively, that constitute a communication link. For a fixed position of, e.g., receiving antenna j , the channel coefficient α_{ij} due to multipath fading can be evaluated for any position of the transmitter i in the environment as a Rayleigh distributed random variable. The values of α_{ij} for different positions of the antenna i are correlated if they are closer than $\lambda/2$ apart, and are independent if they are farther than $\lambda/2$ apart. Therefore, for a fixed position of the receiver j , we can create a spatial map that returns the time average channel gain due to multipath fading for any position of the transmitter i in the environment; see Fig. 2.

¹Typically, Rayleigh fading is used to model situations where no dominant path of wave propagation exists, i.e., line of sight. When line of sight between transmitter and receiver exists, Rician fading is more appropriate. In this paper, we employ Rayleigh fading due to its simpler form.

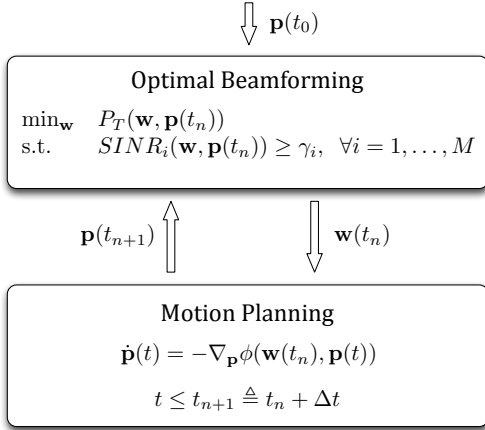


Fig. 3. Joint beamforming and mobility control.

III. INTEGRATED BEAMFORMING AND MOBILITY CONTROL

Given a fixed spatial configuration of the source, relay and destination nodes, the matrices \mathbf{R}_T and $\mathbf{Q}^{(i)}$ in (11) containing the channel gains are fixed and the solution to (11) will return the best beamforming matrix \mathbf{X} that minimizes the sum transmit power at the relays, while maintaining desired SINR at the destinations. While important, this formulation does not take into account the effect that node configuration has on the optimal solution. Our goal in this paper is to solve (11) jointly in the space of communications, i.e., beamforming weights, and node positions. For this, we assume that the source and destination nodes are stationary, while the relay nodes can move. In particular, we denote by $\mathbf{p}_j \in \mathbb{R}^2$ the position of relay node j , which reacts to the control input $\mathbf{u}_j \in \mathbb{R}^2$ according to the first order differential equation

$$\dot{\mathbf{p}}_j = \mathbf{u}_j, \quad j = 1, \dots, K. \quad (13)$$

Introducing dependence of the channel gains, that appear in the matrices \mathbf{R}_T and $\mathbf{Q}^{(i)}$, on the positions of the relays [c.f. (12)], i.e.,

$$f_{ij}(\mathbf{p}_j) = \alpha_{ij}(\mathbf{p}_j) \frac{e^{j(2\pi/\lambda)d_{ij}(\mathbf{p}_j)}}{d_{ij}(\mathbf{p}_j)^{\mu/2}}$$

(similarly for $g_{ji}(\mathbf{p}_j)$), our goal in this paper is to determine motion controllers $\mathbf{u}_j, \forall j = 1, \dots, K$ and a beamforming matrix \mathbf{X} that ensure feasibility of optimization problem (11) as well as minimization of the total transmitted power by the relay antennas at all times.

A. The Proposed Hybrid Controller

Since mobility introduces nonlinearities in (11), we propose a parallel control scheme, where motion control and control of the beamforming variables are performed simultaneously at different time scales. Integration of the two gives rise to a hybrid control scheme, where the discrete time beamforming decisions become the switching signal in the continuous time motion controllers, as shown in Fig. 3.

In particular, while the relays are stationary, the solution to problem (11) provides the optimal beamforming weights. Given those fixed beamforming weights, the relays then move according to (13) for a time interval $\Delta t > 0$ aiming to further decrease the sum transmit power, while maintaining the SINR constrains.

Introducing an additional collision avoidance specification, we can obtain motion controllers \mathbf{u}_j with the desired behavior as the negative gradient of appropriately chosen artificial potential functions $\phi: \mathbb{R}^{2K} \rightarrow \mathbb{R}_+$ such that

$$\phi(\mathbf{p}) \triangleq \phi_{P_T}(\mathbf{p}) + \phi_{SINR}(\mathbf{p}) + \phi_{col}(\mathbf{p}), \quad (14)$$

where $\mathbf{p} \in \mathbb{R}^{2K}$ is the stack vector of all relay positions. The potential

$$\phi_{P_T}(\mathbf{p}) \triangleq Tr(\mathbf{X}\mathbf{R}_T(\mathbf{p})). \quad (15)$$

captures the optimization objective (11) and serves to steer the relays towards spatial configurations that minimize the sum transmit power. Similarly, the potential

$$\phi_{SINR}(\mathbf{p}) \triangleq \sum_{i=1}^M \left[\left(Tr(\mathbf{X}\mathbf{Q}^{(i)}(\mathbf{p})) \right)^2 - 1 \right]^{-1}. \quad (16)$$

aims to enforce feasibility of the SINR constraints (11) throughout the duration of motion of the relays. It does so by creating a “barrier” close to the boundary of the cone \mathbb{R}_+^M , thus, preventing the M constraints $Tr(\mathbf{X}\mathbf{Q}^{(i)}(\mathbf{p})) \geq 1$ from approaching this boundary. The motivation for this potential stems from the well known theory of barrier (interior point) methods used in constrained optimization. Finally, the potential

$$\phi_{col}(\mathbf{p}) \triangleq \sum_{j=1}^K \sum_{k=1, k \neq j}^{2M+K} \frac{1}{\|\mathbf{p}_j - \mathbf{p}_k\|_2^2} \quad (17)$$

is added to ensure collision avoidance among nearby nodes for practical considerations. Then, the controller for every relay j becomes $\mathbf{u}_j = -\nabla_{\mathbf{p}_j} \phi$ and stacking all controllers in a common vector we obtain the centralized closed loop system

$$\dot{\mathbf{p}} = -\nabla_{\mathbf{p}} \phi, \quad (18)$$

which simultaneously enforces satisfaction of the SINR constraints in (11) and steers the relay nodes towards minimizing their total transmitted power. Since the potential ϕ is a non-convex function of the relay positions \mathbf{p} , the proposed approach can only guarantee convergence to a local minimum in the configuration space. Nevertheless, satisfaction of the SINR constraints can be theoretically guaranteed, leading to the following result.

Proposition 3.1: Given beamforming variables, assume the relays move according to the closed loop system (18). Then, if the SINR constraints are initially satisfied, they will be satisfied for all time. (Similarly for collision avoidance.)

Proof: The proof of this result is straightforward and relies on positive invariance of the level sets $\phi^{-1}([0, c]) = \{\mathbf{p} \mid \phi(\mathbf{p}) \leq c\}$ of the artificial potential ϕ , which is due to the fact that $\dot{\phi}(\mathbf{p}) = \nabla_{\mathbf{p}} \phi(\mathbf{p}) \dot{\mathbf{p}} = -\|\nabla_{\mathbf{p}} \phi(\mathbf{p})\|^2 \leq 0$, by equation (18). Since, by construction of ϕ , violation of

the SINR constraint or collisions between nodes imply that $\phi \rightarrow \infty$, we conclude that if the constraints are initially satisfied, they will be satisfied for all time. ■

Proposition 3.1 implies that feasibility of the SINR constraints is maintained between consecutive solutions of problem (11), thus (11) will always be feasible at the time instants when the beamforming weights are computed. Therefore, the hybrid system shown in Fig. 3 ensures feasibility of the SINR constraints for all time. In view of Proposition 3.1, it also ensures collision avoidance. Finally, the proposed integrated system, locally minimizes the sum transmit power at the relays. While it is difficult to provide theoretical guarantees or performance bounds for this, it is shown in simulations that the power savings by employing joint beamforming and position optimization can be significant.

Remark 3.2: It can be easily shown that the inequality constraint in (11) is always active at the optimum (satisfied with equality), for otherwise, the optimal \mathbf{X} could be scaled down to satisfy the constraint with equality, thereby decreasing the objective function and contradicting optimality. This means that the barrier potential (16) will be infinite after each optimization step. In order to overcome this irregularity, we introduce a small slack $\epsilon > 0$ in the potential (16) so that $\phi_{SINR}(\mathbf{p}) \triangleq \sum_{i=1}^M \left[\left(Tr(\mathbf{X}\mathbf{Q}^{(i)}(\mathbf{p})) \right)^2 - (1 - \epsilon)^2 \right]^{-1}$ instead. The practical implications of such a formulation are negligible, as can be seen in section IV.

IV. NUMERICAL ANALYSIS

In this section we illustrate our approach in nontrivial numerical simulations. We consider a scenario with $M = 2$ source-destination pairs, having negligible direct communication links. We employ distributed beamforming with $K = 5$ relay nodes, which are controlled according to the hybrid scheme discussed in Section III and shown in Fig. 3. The channel gains between any two nodes are calculated as in (12). More specifically, we choose the path loss exponent to be $\mu = 3.5$ and the signal wavelength to be $\lambda = c/f = (3 \cdot 10^8)/(2.4 \cdot 10^9) = 0.125\text{m}$. These are reasonable values for mobile robotics applications utilizing ultra high frequency carrier waves (2.4GHz) for wireless transmissions.

For the scenario examined, we build $2M = 4$ multipath fading maps as in Remark 2.1, one for every fixed source and destination. We further set the transmission power of each source at 20 dBm (100mW), where dBm accounts for the ratio in decibels (dB) of the measured power referenced to one milliwatt, define the target SINR values for both destinations at $\gamma_1 = \gamma_2 = 7$ dB and randomly place the relay nodes in the vicinity of the sources. The evolution of the proposed hybrid system is shown in Fig. 4, where the contours represent the spatial average of the $2M = 4$ multipath fading maps, one for every source and every destination.

We observe that the proposed algorithm drastically reduces the required sum transmit power at the relays and, moreover, it does so in a rather monotonic way between consecutive solutions of the optimization problem (11). In fact, starting

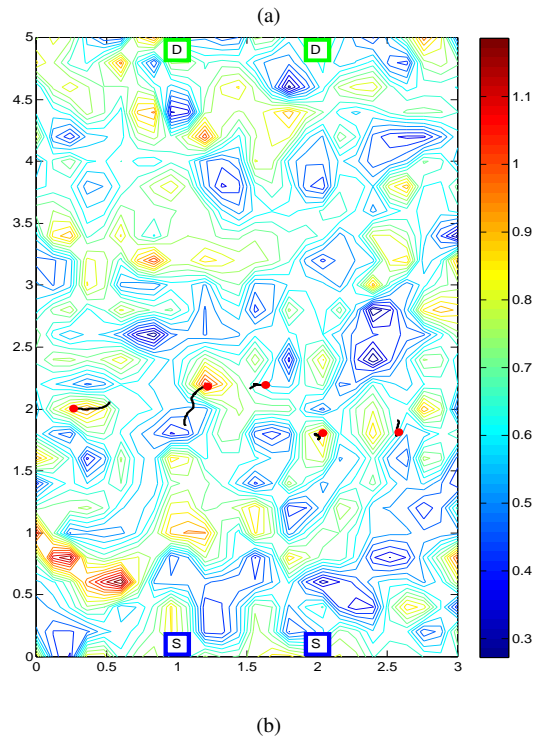
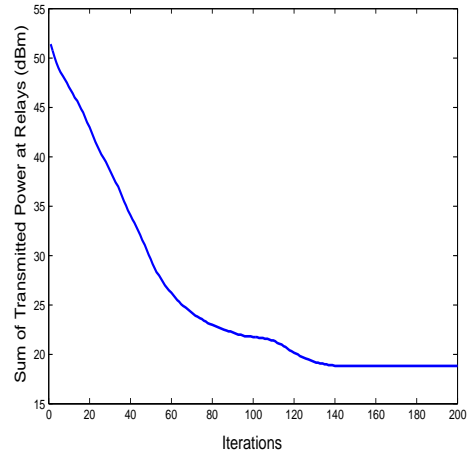


Fig. 4. a) Evolution during motion of the total transmission power required by the relay antennas to achieve the targeted SINR of 7dB at both sources. Here iterations denote the consecutive calculations of the optimization problem (11) b) Evolution of the spatial configuration of the mobile network during application of the proposed control scheme. Blue and green squares denote sources and destinations, respectively. The black, solid lines and red circles denote the trajectories and final positions of the relay nodes, respectively. Also plotted are the contours of the average of the Rayleigh coefficients magnitudes, as mentioned in text.

from an energy inefficient configuration that requires a total power 52 dBm ($\approx 100\text{W}$), our algorithm produces a final spatial configuration that requires only 18 dBm ($\approx 75\text{mW}$) divided among the 5 relay transmitters. Note that in the scenario under consideration the average relay distances from the sources and destinations are between 2 and 3m, thus returning very small values for the path loss coefficient. Therefore, 18 dBm is a quite low final sum transmit power, considering the 7 dB SINR requirement. Finally, note that the

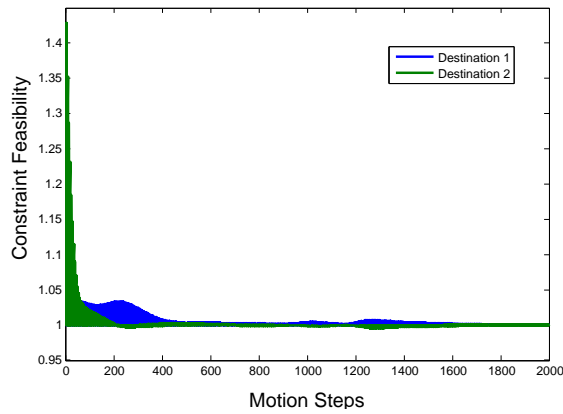


Fig. 5. Evolution of the constraint functions $Tr(\mathbf{XQ}^{(i)})$ values during motion.

relay nodes approach the peaks of the Rayleigh coefficient map to maximize the channel gain due to multipath fading; see Fig. 4. Nevertheless, they do not converge to the peaks, as path loss is also important.

To check whether the SINR constraints at the destinations are satisfied, we plot the function $Tr(\mathbf{XQ}^{(i)})$ as the relays move; see Fig. 5. In view of the slack $\epsilon = 0.1$ that is present in the potentials (16) – see also Remark 3.2 – we see that the SINR constraints are satisfied, as desired. The final beamforming weights obtained using randomization to get a rank one approximation of the optimal beamforming matrix \mathbf{X} [23], for the scenario depicted in Fig. 4, are $\mathbf{w} = [0.1323 - 0.3072i, 0.5984 - 0.4024i, 0.3404 + 0.3490i, 0.5611 - 0.3396i, -0.3665 - 0.4021i]$. These include the optimal amplification and phase shift that the relay nodes (at their optimal configuration) need to apply to their received signals in order to achieve a sum transmit power of 18 dBm.

V. CONCLUSIONS

Maintaining reliable communications in networks of wireless nodes plays a vital role for the accomplishment of most cooperative tasks. Unlike recent approaches that rely on multi-hop communication for information propagation, we employ collaborative beamforming due to its ability to transmit signals over long distances with minimal number of hops, while significantly reducing power consumption and interference levels. The contribution of this work is a novel approach that jointly optimizes the communication variables and the node positions. Our integrated system was shown to exhibit superior performance in terms of power savings compared to approaches that do not consider node mobility. This makes our approach very promising for further research and application in mobile wireless networks.

REFERENCES

[1] A. Jadbabaie, J. Lin, and A. S. Morse, “Coordination of groups of mobile autonomous agents using nearest neighbor rules,” *IEEE Transactions on Automatic Control*, vol. 50, no. 2, pp. 169–182, February 2005.

[2] W. Ren and R. W. Beard, “Consensus seeking in multi-agent systems under dynamically changing interaction topologies,” *IEEE Transactions on Automatic Control*, vol. 50, no. 5, pp. 655–661, May 2005.

[3] I. Stojmenovic, A. Nayak, and J. Kuruvila, “Design guidelines for routing protocols in ad hoc and sensor networks with a realistic physical layer,” *IEEE Communications Magazine*, vol. 43, pp. 101–106, March 2005.

[4] A. Neskovic, N. Neskovic, and G. Paunovic, “Modern approaches in modeling of mobile radio systems propagation environment,” *IEEE Communications Surveys*, vol. 3, no. 3, pp. 1–12, 2000.

[5] Y. Kim and M. Mesbahi, “On maximizing the second smallest eigenvalue of a state-dependent graph laplacian,” *IEEE Transactions on Automatic Control*, vol. 51, no. 1, pp. 116–120, January 2006.

[6] M. Ji and M. Egerstedt, “Coordination control of multi-agent systems while preserving connectedness,” *IEEE Transactions on Robotics*, vol. 23, no. 4, pp. 693–703, August 2007.

[7] M. M. Zavlanos and G. J. Pappas, “Potential fields for maintaining connectivity of mobile networks,” *IEEE Transactions on Robotics*, vol. 23, no. 4, pp. 812–816, August 2007.

[8] M. Schuresko and J. Cortes, “Distributed motion constraints for algebraic connectivity of robotic networks,” *Journal of Intelligent and Robotic Systems*, vol. 56, no. 1, pp. 99–126, September 2009.

[9] E. Stump, A. Jadbabaie, and V. Kumar, “Connectivity management in mobile robot teams,” in *Proc. IEEE International Conference on Robotics and Automation*, Pasadena, CA, May 2008, pp. 1525–1530.

[10] D. P. Spanos and R. M. Murray, “Motion planning with wireless network constraints,” in *Proc. 2005 American Control Conference*, Portland, OR, June 2005, pp. 87–92.

[11] A. Ephremides, “Energy concerns in wireless networks,” *IEEE Trans. on Wireless Communications*, vol. 9, no. 4, pp. 48–59, August 2002.

[12] A. Ribeiro, Z.-Q. Luo, N. D. Sidiropoulos, and G. B. Giannakis, “Modelling and optimization of stochastic routing for wireless multihop networks,” in *Proc. 26th Annual Joint Conference of the IEEE Computer and Communications Societies (INFOCOM)*, Anchorage, Alaska, May 2007, pp. 1748–1756.

[13] A. Ribeiro, N. D. Sidiropoulos, and G. B. Giannakis, “Optimal distributed stochastic routing algorithms for wireless multihop networks,” *IEEE Transactions on Wireless Communications*, vol. 7, no. 11, pp. 4261–4272, November 2008.

[14] M. M. Zavlanos, A. Ribeiro, and G. J. Pappas, “Mobility and routing control in networks of robots,” in *Proc. 2010 49th IEEE Conference on Decision and Control (CDC)*, Atlanta, GA, December 2010, pp. 7545–7550.

[15] H. Gharavi and K. Ban, “Multihop sensor network design for wideband communications,” *Proc. IEEE*, vol. 91, no. 8, pp. 1221–1234, August 2003.

[16] H. Ochiai, P. Mitran, H. V. Poor, and V. Tarokh, “Collaborative beamforming for distributed wireless ad hoc sensor networks,” *IEEE Trans. Signal Process.*, vol. 53, no. 11, pp. 4110–4124, Nov. 2005.

[17] R. Mudumbai, U. Madhoo, D. R. Brown, and H. V. Poor, “Distributed transmit beamforming: Challenges and recent progress,” *IEEE Commun. Mag.*, vol. 47, no. 2, pp. 102–110, Feb. 2009.

[18] L. Dong, A. Petropulu, and H. Poor, “A cross-layer approach to collaborative beamforming for wireless ad hoc networks,” *IEEE Trans. Signal Proc.*, vol. 56, no. 7, pp. 2981–2993, July 2008.

[19] J. Li, A. Petropulu, and H. Poor, “Cooperative transmission for relay networks based on second-order statistics of channel state information,” *IEEE Trans. Signal Proc.*, vol. 59, no. 3, pp. 1280–1291, March 2011.

[20] Y. Liu and A. Petropulu, “Cooperative beamforming in multi-source multi-destination relay systems with sinr constraints,” in *Proc. 2010 IEEE Conference on Acoustics Speech and Signal Processing (ICASSP)*, Dallas, TX, March 2010, pp. 2870–2873.

[21] L. Vandenberghe and S. Boyd, “Semidefinite programming,” *SIAM Review*, vol. 38, no. 1, pp. 49–95, 1996.

[22] S. Boyd and L. Vandenberghe, *Convex Optimization*. Cambridge University Press, 2004.

[23] N. Sidiropoulos, T. Davidson, and Z. Luo, “Transmit beamforming for physical-layer multicasting,” *IEEE Trans. Signal Proc.*, vol. 54, no. 6, pp. 2239–2251, June 2006.

[24] B. Sklar, “Rayleigh fading channels in mobile digital communication systems - part I: Characterization,” *IEEE Communications Magazine*, vol. 35, no. 7, pp. 136–146, July 1997.